Scientific Research Publishing

American Journal of Plant Sciences, 2026, 17(3), 251-271
https://www.scirp.org/journal/ajps
ISSN Online: 2158-2750
ISSN Print: 2158-2742

Characterization, *in Vitro* and *in Silico* Approach for the Management of Nigrospora Leaf Blight Disease of Guava in Bangladesh

Md. Maniruzzaman Sikder*, Md. Sabbir Ahmmed, Beauty Akter, Nusrat Binte Alam, Md. Nazmussakib Shuvo, Sayma Sajuti, Farhana Rahman, Nuhu Alam

Department of Botany, Jahangirnagar University, Savar, Bangladesh
Email: *mmsbot@juniv.edu

How to cite this paper: Sikder, M.M., Ahmmed, M.S., Akter, B., Alam, N.B., Shuvo, M.N., Sajuti, S., Rahman, F. and Alam, N. (2026) Characterization, *in Vitro* and *in Silico* Approach for the Management of Nigrospora Leaf Blight Disease of Guava in Bangladesh. *American Journal of Plant Sciences*, **17**, 251-271.
https://doi.org/10.4236/ajps.2026.173017

Received: December 2, 2025
Accepted: March 21, 2026
Published: March 24, 2026

Abstract

The current study was conducted to detect the pathogenic fungus causing leaf blight disease of guava in Bangladesh, and to evaluate the effect of various physical factors on the fungal growth, *in vitro* disease management, and the prediction of potential phyto-compounds against the fungus through *in silico* technique. The fungus was isolated following the tissue planting method, and morphological and molecular characterization confirmed the fungal identity as *Nigrospora chinensis*. *In vitro* pathogenicity tests ascertained the pathogenic nature of the fungus. The optimum fungal growth was found on PDA medium at 25˚C temperature and pH 7 conditions. Among three commercial fungicides—Amistar top 325 SC and Kazim 80 WG showed complete growth inhibition of the fungus, and fungal antagonist *Trichoderma harzianum* showed above 70% growth inhibition in *in vitro* dual culture. The virtual screening results for the target protein Tef-1 revealed that seven phytocompounds had a higher binding affinity. Among them, lawsaritol of *Lawsenia inermis* and andrograpanin of *Andrographis paniculata* showed the highest outcomes (binding affinity −7.5 and −11.4 kcal mol^{-1}) than the control chemical fungicide carbendazim. The average root-mean-square deviation (RMSD) value of the protein backbone regarding lawsaritol, andrograpanin, and carbendazim was 2.588 Å, 1.807 Å, and 2.026 Å, respectively, and the root mean square fluctuation (RMSF) values were 3.89 Å, 5.65 Å, and 4.51 Å during molecular dynamic simulation. *In silico* studies reveal that two compounds can be potential biogenic fungicides against the concerned disease caused by *N. chinensis*. To the best of our knowledge, leaf blight disease of guava and *in silico* drug prediction against the fungus are reported for the first time in Bangladesh.

Keywords

Fungal Blight, Molecular Identification, Growth Characteristics, Computer-Aided Drug Design

1. Introduction

Bangladesh is one of many South Asian countries sometimes recognized as fruit center with almost 50 different species. Guava (*Psidium guajava* L.) is an important horticultural crop in this country that has a high demand in the domestic market due to its high dietary fiber, sweetness, vitamin abundance [1] [2]. Guava leaves are often explored for their therapeutic and curative properties which include antidiarrheal, antimicrobial, anticancer, antidiabetic and lipid-lowering effects [3]. Nutritional and physicochemical analysis revealed that mature and ripened guava fruit contains very lucrative amounts of reducing sugar, crude fiber, carbohydrate, protein, vitamin C, sodium, potassium, iron etc. and hence it's called the apple of poor people [4]. In Bangladesh, although kazi peyara is the most commercially available variety, other varieties such as Swarupkhathi-1 and 3, Lal peyara, Kushum peyara, BARI Peyara 1-4, BAU peyara 1-6, IPSA Peyara-1 etc. are also grown in homestead and on a commercial basis [5]. Being a highly renumerative crop, the importance of its illness cannot be underrated. Wilt of guava is an important disease caused by several pathogenic fungi viz., *Fusarium oxysporum* f. sp. *psidii*, *F. chlamydosporum*, *F. solani* and *F. proliferatum* [6] [7]. Several other diseases of guava plants have also been reported viz., stylar end rot by *Lasiodiplodia pseudotheobromae* [8]; fruit rot by *F. semitectum* and *Phytophthora nicotianae* [9] [10]. *Pestalotiopsis* spp. was reported to cause scab disease of guava in Hawaii [11]. In Saudi Arabia, post-harvest spoilage of guava fruits was reported to be caused by *Botryodiplodia theobromae* [12]. *Nalanthama psidii*, *Phyllostica capitalensis*, and *Colletotrichum tropicale* causing wilt, black spot, and anthracnose diseases of guava were reported in China and Mauritius [13]-[15]. In Malaysia, fruit rot disease of guava caused by *Neoscytalidium dimidiatum* and *Lasiodiplodia theobromae* was reported [16] [17].

Drug resistance develops because of fungicide exposure over an extended period. It has also been demonstrated that these fungicides pose a significant risk to human health and the environment [18]. Novel scaffolds are therefore required to reduce drug resistance and safeguard crop productivity. Many countries and societies have old cultures and traditions that reference the healing value of plant compounds, which are also considered safe and reasonably priced and have been utilized for thousands of years as a base for traditional medicine [19] [20]. Numerous studies led to the screening of numerous plant species and bioactive chemicals for their antibacterial properties, which produced the discovery of structurally distinct biologically active compounds [21]. Computational techniques can be applied to their target identification.

The translation elongation factor (TEF) 1 alpha gene is responsible for encoding a crucial component of the protein translation machinery, particularly in different organisms [22]. To tackle phytopathogenic fungi, natural inhibitors of the target protein are needed, as synthetic fungicides might be harmful to the environment. The purpose of this study was to evaluate the antifungal efficacy of certain plant components against the guava phytopathogenic fungus. The inhibitory effect of several bioactive plant chemicals against the TEF-1 enzyme was also investigated using molecular docking. The chosen compounds underwent drug-likeness testing to evaluate their pharmacological efficacy and dependability. Finally, a molecular dynamics simulation investigation was done to identify an energetically stabilized complex involving the target protein.

In Bangladesh, no previous research work has been conducted on leaf blight disease of the guava plant. Therefore, the present work aimed to study the symptomatology, isolation, identification, *in vitro* characterization, and management of the fungi causing guava leaf blight disease as well as to carry out computer-aided prediction to uncover potential antifungal phytocompounds against the fungal pathogen.

2. Materials and Methods

2.1. Study Area, Field Observation, and Symptomatology

The fieldwork was conducted in three rooftop gardens and three nurseries located around Jahangirnagar University, Savar, Dhaka, Bangladesh. Three plants of each sampling area were observed for the appearance of disease symptoms. During July to September 2023, disease symptoms were recorded and characterized following standard phytopathological manual.

2.2. Sample Collection and Fungus Isolation

Infected leaves of guava with distinct blight symptoms were collected in sterile polyethylene bags from the rooftop gardens and nurseries. From each location, three diseased leaves with similar symptoms were collected for further investigations. Necessary photographs were taken and samples were cut into pieces at 2 mm diameter. Samples were then surface sterilized with 5% sodium hypochlorite for 3 minutes, followed by washing 3 - 4 times in sterilized distilled water. After surface drying, samples were immediately transferred into petri-dishes containing sterilized Potato Dextrose Agar (PDA) medium, then the plates were incubated at room temperature (25˚C ± 2˚C) for 3 - 5 days. After the fungal appearance, it was subsequently transferred to fresh PDA medium following fungal tip culture [23].

2.3. Identification of the Fungus and Test of Pathogenicity

Morphological and molecular methods were used to identify the fungus. Visual characteristics like colony color, appearance, mycelium and reproductive struc-

tures were recorded for morphological identification. Molecular identification was done by analyzing the internal transcribed spacer (ITS) sequence although multilocus sequence analysis could be used for more precise detection. Fungal DNA isolation was isolated according to standard protocol and PCR were performed using ITS1 and ITS4 primer sets. DNA sequencing was performed in the First Base Laboratories, Sdn Bhd, Malaysia by commercial service provider. National Center for Biotechnology Information (NCBI) BLASTn search with the nucleotide sequence data were conducted for similarity indexing. The evolutionary history of the fungus was inferred by using the Neighbor-joining method and the Tamura 3-parameter model derived from the ITS1/5.8S rDNA/ITS2 sequence [11]. Evolutionary analyses were conducted in MEGA (version 12.1) software [24]. *In vitro* pathogenicity test was carried out following detached leaf technique to confirm Koch's Postulates. Healthy and susceptible leaves of guava were detached from plants and subsequently were surface sterilized with cotton soaked 70% ethanol. After that leaves were placed on petri-dishes containing sterilized water soaked blotting paper to maintain moisture condition. Artificial wounds were made using sterilized needle on the leaves and 5 mm mycelial disc from actively growing fungal culture were inoculated onto the wounded leaves. Agar plug without fungus was also inoculated as control. The inoculated plates were placed into vacuumed desiccator at room temperature for 7 days. Three replications of each treatment were maintained during this experiment. Fungal pathogen was re-isolated and characterized from artificially produced diseased tissues.

2.4. *In Vitro* Physiological Study

To determine the optimum temperature for the fungal growth, sterilized Potato Dextrose Agar (PDA) medium was used and each petri plate was inoculated with a 2 mm diameter active growing fungal disc at the center. Inoculated petri plates were incubated at 15˚C, 20˚C, 25˚C, 30˚C, and 35˚C temperature. To evaluate the effect of H^+-ion concentration on the fungal growth, pH of PDA medium was adjusted to five different levels viz., 5.0, 6.0, 7.0, 8.0 and 9.0 by calibrated digital pH meter using sterile 1 M HCl or 1 M NaOH solution before autoclave. The inoculated plates were incubated in a controlled environment. The effect of seven different fungal culture media (MA: Malt Agar; HPA: Honey Peptone Agar; HEA: Host Extract Agar; SGA: Sucrose Dextrose Agar; PDA: Potato Dextrose Agar; PSA: Potato Sucrose Agar; CA: Carrot Agar) was also examined to observe the growth response of the fungus. In all the cases, radial mycelial growth was recorded using millimeter scale after 7 days of incubation.

2.5. Disease Management

2.5.1. *In Vitro* Control Measures

In the current study, three commercially available fungicides, namely—Kazim 80 WG (carbendazim), Copper blue 50 WG (copper oxychloride), and Amistar

top 325 SC (azoxystrobin + difenoconazole) were evaluated at different concentrations (ppm) against the radial growth of the pathogenic fungus following food poison technique. Besides, two *Trichoderma* species (*T. harzianum* and *T. erinaceum*) were employed to assess their efficacy against the fungal isolate following the dual culture technique. Petri plates with untreated PDA medium were used as control. Data on radial growth were recorded after 7 days of post-incubation (dpi), and the following method was used to calculate the percent growth inhibition:

$$I = \frac{C - T}{C} \times 100$$

Here, I = Percent growth inhibition; C = Growth of fungus on control plate; T = Growth of fungus on treatment plate.

2.5.2. *In Silico* Drug Prediction Against the Fungus

The selection of effective phytocompounds through virtual screening and the development of biogenic compounds from selective plants against the target pathogen using *in silico* approaches were conducted during this study [25].

1) Target protein modeling, 3D structure refinement, and validation

Translation elongation factor 1-alpha (Tef-1*α*) is essential for protein synthesis and usually present as a single-copy, highly conserved gene, so silencing it strongly impairs fungal growth. For this reason, the protein was selected as a target protein of our study [26], and the FASTA sequence of the protein was retrieved from the UniProt website (https://www.uniprot.org/) (Entry: A0A8E6NX89) [27]. The 3D structure of the Tef-1 *α* protein was generated using the selected sequence through Ab initio modeling [28]. The GalaxyTBM server (https://galaxy.seoklab.org/cgi-bin/submit.cgi?type=TBM) was used in this purpose. The Tef-1*α* 3D structure was refined using Galaxy Refine server (https://galaxy.seoklab.org/cgi-bin/submit.cgi?type=REFINE) [29]. The best structure was chosen based on GDT-HA, RMSD, MolProbity score, clash score, weak rotamers, and Rama preference. The Ramachandran plot provides relevant information and ratios regarding the anticipated residual structure in protein models within favored, permitted, and disallowed regions [30].

2) Virtual screening for phytocompounds

In this study, ten phytocompounds from two common medicinal plants in Bangladesh were carefully chosen based on their antifungal activity. The 3D structures of these compounds were retrieved in SDF format from the PubChem database (https://pubchem.ncbi.nlm.nih.gov/) and converted them into PDB format using Open Bable [31] [32].

3) Molecular docking

a) Protein and ligand preparation

The protein and ligand structures were prepared for docking using MGL tools and saved as PDBQT format [33]. The energy minimization of both protein and ligand was done by UCSF Chimera software [34].

b) Active site prediction, grid box preparation, and docking

Pharmacology studies show that the functional activity of a protein is terminated if ligands bind in the active site of the protein [35]. The active site in the target protein was predicted by the CASTp server (http://sts.bioe.uic.edu/castp/) [36]. Moreover, docking methods determine the conformations assumed around the binding sites of macromolecular targets and calculate the ligand-receptor's binding free energy [37]. The centre of the grid box was placed at the coordinates X = 25.735 Å, Y = 30.988 Å and Z = 30.846 Å, and it covers most of the binding sites of the protein. The dimensions were X = 60 Å, Y = 60 Å and Z = 60 Å, with a spacing of 0.375 between each grid point. The exhaustiveness value was 8. All docking was performed using AutoDock Vina and the 2D diagram of complexes was visualized using Discovery Studio 2021 to recognize the interactions (hydrogen bonds, electrostatic interactions, and hydrophobic interactions) of the amino acids between protein and ligand [38] [39].

4) Fungicides likeness

The pharmacokinetic properties of the best promising compounds were checked using SWISS ADME (https://www.swissadme.ch/) [40]. Drug-like ligands should exhibit molecular weight ≤ 500 Da, logP ≤ 5, hydrogen bond donors ≤ 5, and hydrogen bond acceptors ≤10 [41].

5) Molecular dynamics (MD) simulation

To thoroughly assess the binding stability of the protein-ligand complexes, comprehensive MD simulations were performed utilizing Desmond software on a Linux-based operating system. The protein-ligand complex structures were hydrated using the cubic three-point transferable interaction potential (TIP3P) system construction tool. To normalize the constructed model, Na^+ and Cl^- charged ions were added for the formation of the 0.15 M physiological salt. To attain optimal efficacy concerning energy usage, the integrated force field, OPLS3e, was implemented. The simulation was performed employing the isothermal isobaric ensemble (NPT) method, with a temperature set at 310 Kelvin and a pressure of 1.013 bar. The capture interval was 100 ps long and occurred inside the 100 ns time frame. Meanwhile, the trajectory's memory stored a thousand frames.

2.6. Statistical Analysis

All statistical observations were carried out on the mean value of the three replications. Analysis of variance (ANOVA) was subjected to statistical analysis using the data analysis software SPSS (version.20). Mean was separated using DMRT to compare the effects of treatment on the different fungi.

3. Result

3.1. Symptomatology

Nigrospora leaf blight disease symptoms appeared at the tip which were initially brown-colored and later turned into black (**Figure 1(a)**). Primarily, a small ne-

crotic spot was formed, which gradually became large to form an overall blight symptom. As the symptom develops the surrounding tissues and the midrib become yellow and later turn into a deep brown to black necrotic lesion.

3.2. Morphological Studies of the Fungus

On PDA medium, the fungus was found moderate to fast-growing nature with white circular colony. Initially colony texture was floccose to cottony and become dense with age (**Figure 1(b)**). The conidia were globose to sub-globose, single-celled, shiny, smooth, and initially pale brown color. At maturity, the fungus produces abundantly distinct black conidia that often produce dot on the colony surface, giving a peppered appearance. Conidiophores were reduced to conidiogenous cells, which were solitary, ampulliform, or subspherical (**Figure 1(c)**). Based on the recorded characteristics, the fungus was primarily identified as *Nigrospora* sp.

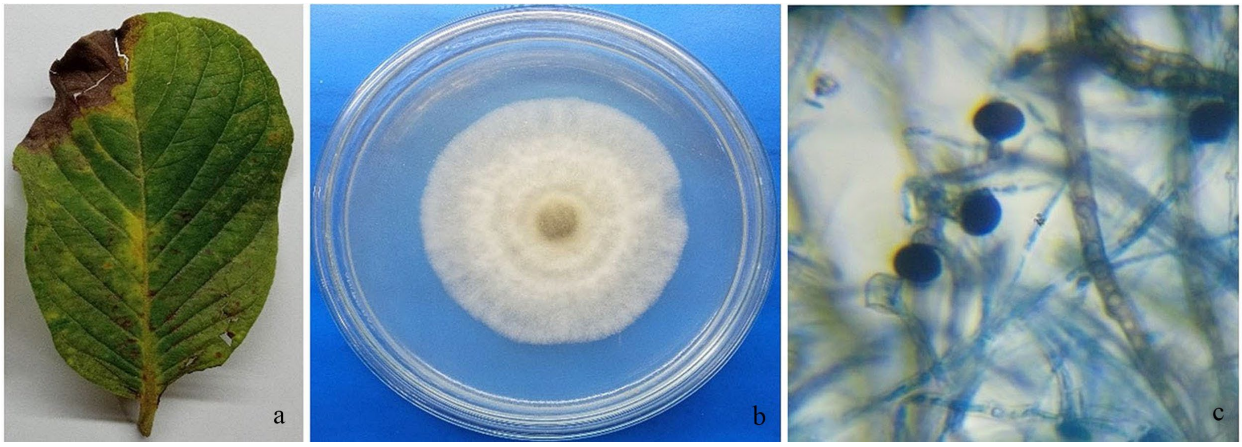

Figure 1. Diseased sample and morphology of the fungus. (a) Leaf blight symptom; (b) Fungal colony on PDA medium; (c) Structure of mycelia, conidia and conidiophore (10 × 40X).

3.3. Molecular Studies of the Fungus

The rDNA-ITS was successfully amplified and the PCR amplicon size was ~555bp after necessary trimming from both ends. A BLASTn analysis of the ITS sequence against NCBI GenBank database revealed a high sequence similarity with closely related taxa. The isolate showed >99% identity and 100% query coverage with other *Nigrospora chininsis* of the database. The sequence alignment led to the creation of a Neighbor-joining tree separates the *N. chinensis* into a distinct clade including our taxa with a strong bootstrap support, thus confirmed the fungal identity as *Nigrospora chinensis* Mei Wang & L. Cai [42] (**Figure 2**). The ITS sequence data was deposited in the GenBank database with the accession number PP442566.1. Successful *in vitro* pathogenicity test confirmed the pathogenic nature of *N. chinensis* to create the disease. The re-isolated fungus produced similar morphological traits during micro-and macro-morphological characterization.

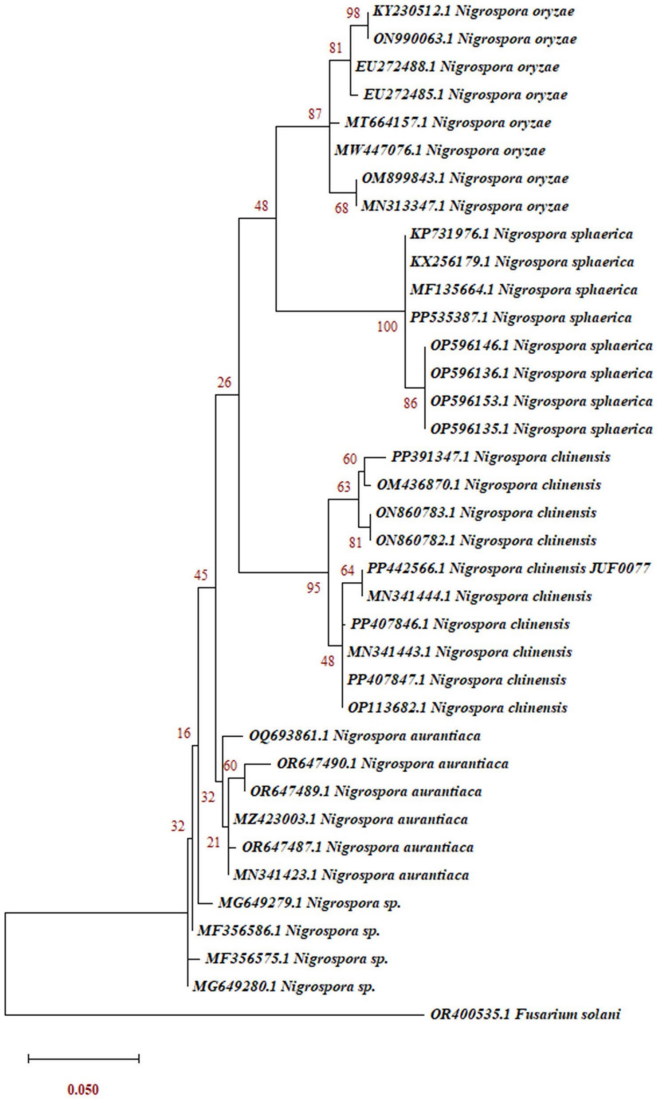

Figure 2. Neighbor-joining tree showing the phylogenetic relationship among the selected fungal isolates including the current taxa (PP442566.1) with 100% bootstrapping.

3.4. Effect of Physical Parameters on Fungal Growth

The growth response of the target fungus was significantly influenced by the investigated parameters, including culture media, media pH and incubation temperature. Results of this study revealed that there is a significant effect of culture media on the mycelial growth of *N. chinensis* ($p < 0.05$), and the highest mycelial growth (73.33 mm) was obtained on PDA medium at 7 dpi followed by HPA, PSA, MA, CA and HEA media (**Figure 3(a)**). The vegetative growth of the fungus was completely ceased at the host extract media. This is maybe due to high concentration metabolic compounds. Data on the effect of pH revealed that the mycelial growth of the fungus was significantly varied by media pH ($p > 0.05$). There was an increasing trend of mycelial growth of *N. chinensis* from pH 5 to pH 7 and it attained the highest diameter of 79.22 mm at pH 7. After reaching the peak the

vegetative growth started declining and the growth was very slow at both lowest and highest tested pH conditions (Figure 3(b)). Significant effect of temperature was found on the growth and development of the fungus. The utmost vegetative growth (90 mm) was recorded at 25˚C, followed by 20˚C, while no growth was found at 15˚C and 35˚C (Figure 3(c)). This might have occurred because of the strain's temperature specificity.

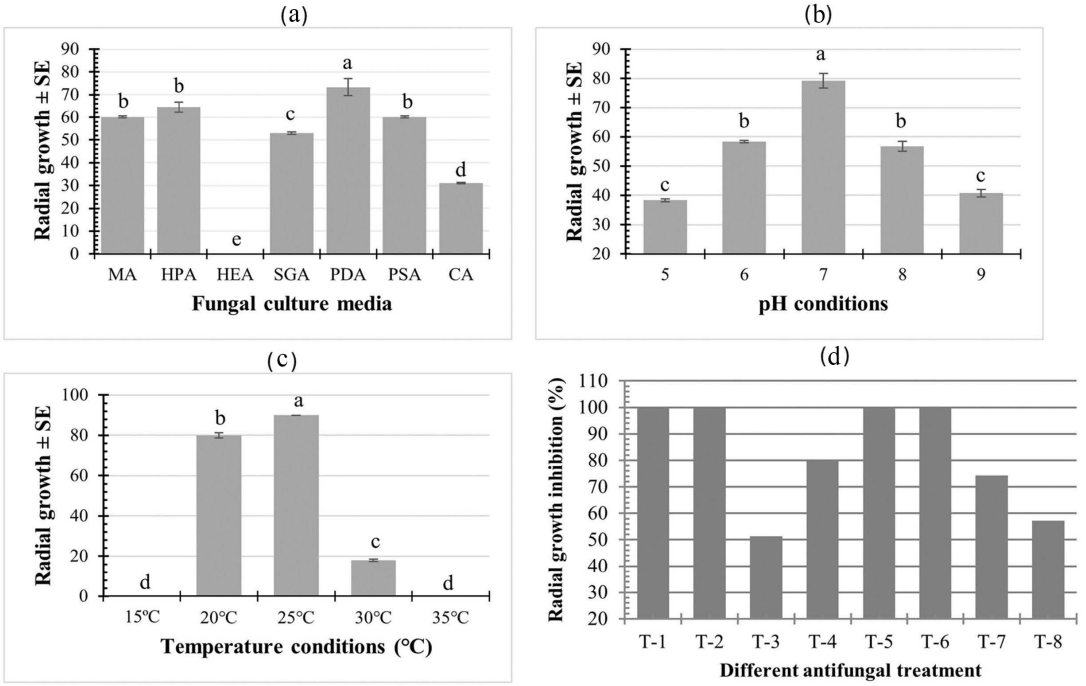

Figure 3. Effect of different factors on the radial vegetative growth of the fungus. (a) Effect of culture media, (b) Effect of pH, (c) Effect of temperature and **d-**Inhibitory effect of different antifungal agents on the radial mycelial growth of *N. chinensis* (T-1: Amistar top 250 ppm, T-2: Amistar top 500 ppm, T-3: Copper blue 1500 ppm, T-4: Copper blue 2000 ppm, T-5: Kazim 500 ppm, T-6: Kazim 1000 ppm, T-7: *T. harzianum* and T-8: *T. erinaceum*). [The same letter denotes no significant difference at $p < 0.05$].

3.5. Disease Management

3.5.1. *In Vitro* Control Measures of the Fungus

The efficacy of selective chemical fungicides and fungal antagonists was evaluated and all of them exhibited varying degrees of growth inhibition with significant differences among treatments. Amistar top at 250 ppm and 500 ppm concentration showed complete growth inhibition of the fungus and Kazim at 500 ppm and 1000 ppm showed a similar inhibitory response (Figure 3(d)). However, copper blue at 1500 ppm and 2000 ppm concentrations showed about 50% and 80% growth inhibitory effects, respectively. The fungal antagonist *Trichoderma* spp. demonstrated substantial inhibitory effects on *N. chinensis* through rapid colonization and overgrowth in the dual culture assay. Between two antagonists, *T. harzianum* showed >70% growth inhibition, followed by *T. erinaceum* (57%), which is often comparable to lower dose of chemical fungicide treatments.

3.5.2. *In Silico* Drug Prediction Against the Fungus

1) 3D Structure Prediction, Validation, Refinement and the binding pocket of the target protein

The GalaxyTBM server was used as the best template to generate the top five models of the target protein Among the five models, model 1 was selected as recommended by the server. Then this protein structure is refined using the GalaxyWEB server. GalaxyWEB generated 5 refined models of the predicted 3D structure of the targeted protein. Among them, model 5 was selected based on an RMSD value of 0.88, MolProbity 0.80, Clash score of 0.9, and Poor rotamers score of 0.0. Validation of the protein structure through the Ramachandran plot from the SAVES server showed 94.5% residues in the favored region (Figure 4). Multiple active sites were assumed by CastP server (sequence no. TRP 35, ILE 72, ALA 108, LEU 184, TYR 13, LEU 17, MET 156, PHE 151).

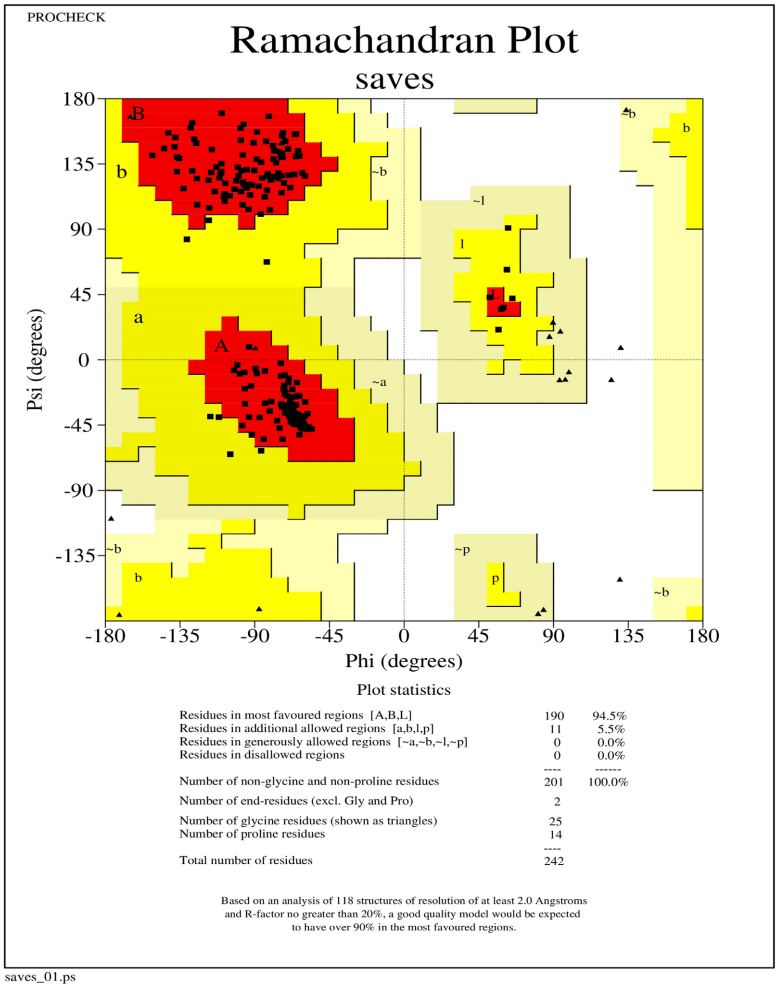

Figure 4. Validation of the 3D structure of the protein. The Ramachandran plot statistics represent the most favorable regions with a percentage of 94.5%.

2) Molecular docking analysis

The target protein contained four active sites marked as pockets where the lig-

ands preferred to dock (Figure 5). Autodock Vina performed docking between the protein and selective ligands to anticipate their binding interactions. Ten phytocompounds were docked with the target protein (Tef-1) and seven were shown to have a higher affinity for binding than the commercial fungicide (carbendazim) which was designated as a control in this study (Table 1).

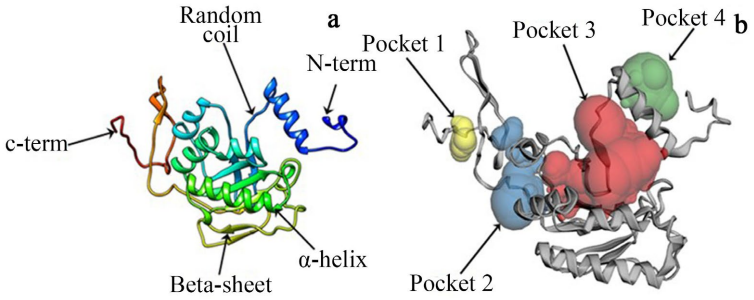

Figure 5. Visualization of the protein. (a) The 3D structure of the selected target protein; (b) Binding sites in the target protein.

Table 1. Docking outcome of selected phytocompounds and control chemical with the target protein. The table shows the binding affinity score of phytocompounds and control chemicals with their sources.

Sl. No	Name of Phytocompounds (Ligand)	Bioaffinity score	Sources
1	Lawsaritol	−7.5	*Lawsenia enermis*
2	Luteolin	−7.4	*Lawsenia enermis*
3	Naphthoquinone	−6.6	*Lawsenia enermis*
4	Lawsone	−7.0	*Lawsenia enermis*
5	Lawsoniaside	−7.0	*Lawsenia enermis*
6	Andrograpanin	−11.4	*Andrographis paniculata*
7	Andrographic acid	−10.8	*Andrographis paniculata*
8	Andrographidin A	−9.6	*Andrographis paniculata*
9	Andrographiside	−10.4	*Andrographis paniculata*
10	Andrographolide	−11.1	*Andrographis paniculata*
11	Carbendazim (Control chemical)	−7.1	Kazim 80 WG

The phytocompounds with higher binding affinity than the control (−7.1) have been selected as the potential fungicide candidate. In this study, seven phytocompounds exhibited better binding affinity score over the control.

3) Fungicide likeness

The SwissADME online program integrates different pharmacokinetic guidelines used for analysis to define leads that will be appropriate for use as an effective antifungal compound. Among the seven phytocompounds, five compounds displayed no signs of breaking the laws governing fungicide likeness (Table 2).

Table 2. Fungicide likeness properties of the selected phytocompounds.

SL No.	Phyto-compound	Molecular weight < 500, g mol^{-1}	Number of H-bond acceptors	Number of H-bond donors	Log $P_{o/w}$	Lipinski Drug likeness	GI absorption
1	Lawsaritol	286.24	6	4	1.73	Yes 0 violation	High
2	Andrograpanin	318.45	3	1	3.30	Yes 0 violation	High
3	Andrographic acid	364.43	6	4	1.27	Yes 0 violation	High
4	Andrographidin A	462.45	10	4	2.64	Yes 0 violation	High
5	Andrographolide	350.45	5	3	2.59	Yes 0 violation	High

4) Visualization of a 2D diagram of the best-hit compounds

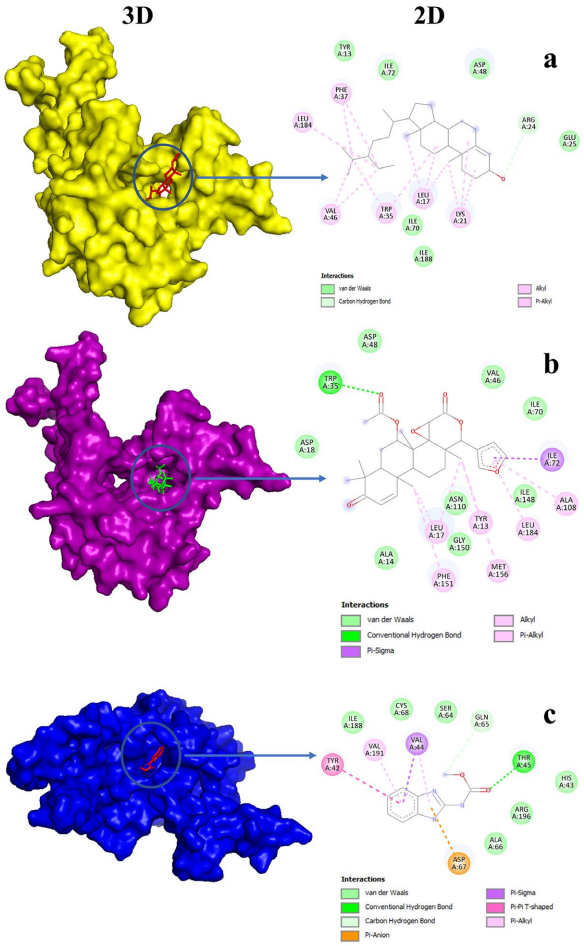

Figure 6. Illustration of 3D and 2D complexes representation. The white circle depicts the binding pockets and includes ligands and target molecules. (a) 3D and 2D interaction of tef-1 with lawsaritol complex. (b) 3D and 2D interaction of tef-1 with andrograpanin complex. (c) 3D and 2D interaction of tef-1 with carbendazim (control) complex.

In the molecular docked complexes, the H-bonds and non-bonded interactions

indicate the stabilization of binding interactions. In this study, Lawsaritol from *L. enermis* and Andrograpanin from *A. paniculata* had the highest binding affinity with tef-1 protein (Table 1). For the protein-lawsaritol complex, the compound forms an H-bond with the amino acid in position 24 of tef-1 (Figure 6(a)). For the protein-andrograpanin complex, the compound forms an H-bond with the amino acid in position 134, 126, 127 of tef-1 (Figure 6(b)). For the protein-control complex, the compound forms an H-bond with the amino acid in position 45 of tef-1 (Figure 6(c)). Afterward, these complexes were run for a stability check through MD simulation.

5) Analysis of the result of the MD simulation

A 100-ns MD simulation was conducted using the two top-performing compounds, lawsaritol, andrograpanin, and the control fungicide carbendazim to verify the stability of the ligands at the active site of the protein. The RMSD, RMSF, hydrogens, and several bonds were assessed. The average RMSD plots of the backbone of Tef-1 protein regarding lawsaritol, andrograpanin, and carbendazim were 2.588 Å, 1.807 Å, and 2.026 Å, respectively (Figure 7(a)). Throughout the remainder of the 100-ns simulation period, the deviation of the curve remained below 3.00 Å. The RMSD of the ligands was more stable than that of the control. The curve of the control was not stable during the 100 ns simulation; in the meantime, the other compounds became stable before 20 ns, and the average RMSD values of the lawsaritol and andrograpanin were 3.023 and 2.935 Å, respectively (Figure 7(b)). The average RMSF value of the protein regarding the ligands was almost the same as the control, 3.89, 5.65, 4.51 Å (Figure 7(c)).

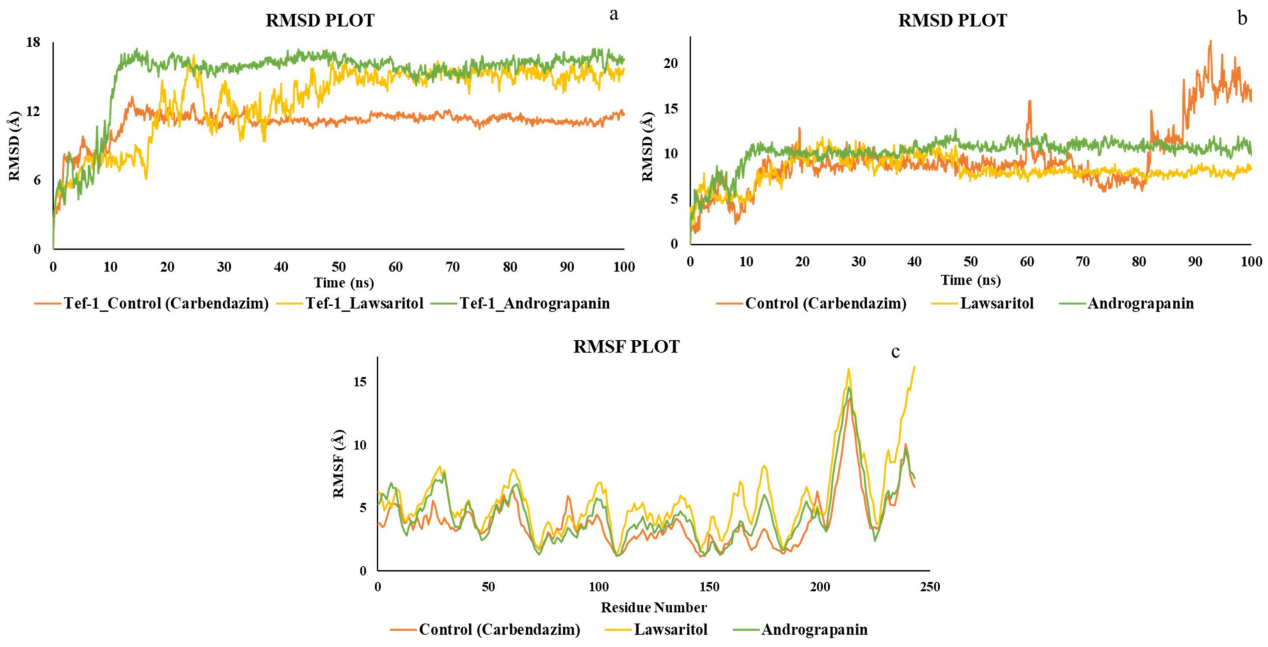

Figure 7. RMSD and RMSF of the protein-ligands complex. The graph demonstrated (a) the RMSD value of the backbone of the protein regarding ligands, (b) the RMSD of the ligands, (c) the RMSF of amino acids of the protein.

The non-covalent interactions between the protein and ligands were evaluated

in the 100-ns simulation period (Figure 8). Regarding lawsaritol, 4 interactions with ARG24, PHE37, ASP48, and PHE151 of the protein lasted more than 20% of the total simulation time. Another ligand, andrograpanin, interacted with 3 (TYR13, TRP35, and ASN110) amino acids of the protein for more than 35% of the simulation period. On the other hand, carbenzadim showed better interaction with THR45 of the protein, and the interaction time was 125% of the simulation. Usually, it happens when ligands interact with the same amino acid several times [43].

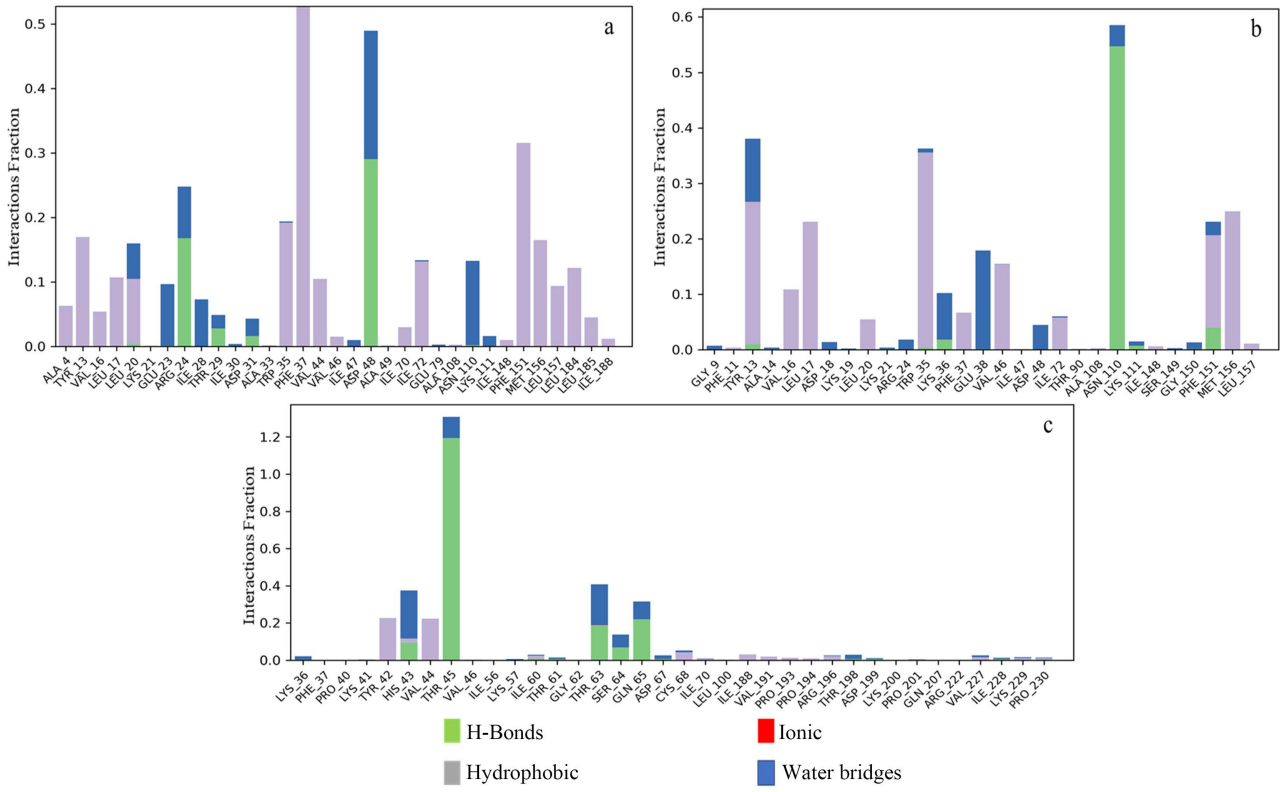

Figure 8. Histogram of the protein-ligand interaction. a, b, and c indicate the interaction of lawsaritol, andrograpanin, and carbendazim, respectively.

4. Discussion

Nigrospora chinensis was found to be the causal organism of leaf blight disease f guava in the current investigation. Morphological and molecular identification techniques confirmed the identity of the fungus, *in vitro* pathogenicity test following the detached leaf technique reconfirmed the pathogenic nature of the fungus. *N. chinensis* was reported to cause leaf blight disease of Camellia oleifera in China [44].

In the current study, among the tested fungal culture media *N. chinensis* revealed its best growth on PDA medium at 25˚C temperature and pH 7 conditions. Profuse fungal growth was observed on the PDA medium, most probably due to the presence of higher dextrose content in it. However, the fungus was unable to show any growth on the host extract agar medium, this could be due to the greater

content of alkaloids and flavonoids in the leaf extracts. Likewise, a previous lab study showed that *N. sphaerica* preferred to grow at 25˚C and pH 7 - 8 conditions [45]. Sempere and Santamarina (2006) [46] also cited that *Nigrospora oryzae* had the highest growth at 25˚C temperature. In China, leaf blight disease of *Cyclocarya paliurus* caused by *N. sphaerica* was reported and the mycelial growth of the fungus was observed at temperatures ranging from 5˚C to 35˚C, where the optimum growth was found between 25˚C and 30˚C [47]. Hence, *Nigrospora* has specificity on suitable temperature and pH conditions.

In the recent research work, all three chemical fungicides viz., Amistar top 325 SC (Azoxystrobin + difenoconazole), Kazim 80 WG (Carbendazim), and Copper blue 50 WG (Copper oxychloride) were found to be the potential to inhibit the fungal growth around the prescribed doses. Besides, *T. harzianum* revealed an outstanding verdict that it could limit the fungal infection at a promising level. In an earlier study, Amistar Top (azoxystrobin + difenoconazole) significantly inhibited the growth of *Colletotrichum falcatum* in all concentartions compared to control, and the radial growth was inhibited by 90% at 50 ppm concentration [48]. Amistar Top 32.5% was recorded the best disease reducing efficacy to downy mildew and purple blotch of onion [49]. Amistar top at a 1000 ppm concentration was found cent percent mycelial growth inhibition of *Fusarium musae,* causing fruit rot disease in banana [50]. *In vitro* study revealed that carbendazim was the most effective fungicide against *N. anhuiensis* with a concentration of 5 μg ml^{-1} [51]. It has also been reported that Carbendazim 50 WP at 1000 ppm and 500 ppm concentration exhibited notable inhibition against *Pyricularia grisea* causing blast disease of pearl millet [52]. Nowadays, it has become a trend to shift toward a healthy, safe, and eco-friendly management package to control fungal pathogens using biocontrol agents. A lab bioassay mentioned that fungal antagonist *T. harzianum* exhibited a promising outcome against *N. sphaerica* [45]. Similarly, *T. harzianum* inhibit the mycelial growth completely of *Sclerotium rolfsii* and *Alternaria* sp., 92.02% for *Aspergillus niger*, 94% for *Fusarium oxysporum*, 100% for *Pythium aphanidermatum* [53]. So, *T. harzianum* could be used as an effective and eco-friendly way to control for leaf blight disease of guava.

Additionally, i*n silico* drug design is reputed for discovering potent inhibitors of several plant diseases. Antimicrobial activity of the phytocompounds of *Vernonia cinerea* has been identified and predicted using *in silico* techniques against *Xanthomonas oryzae* causing bacterial blight disease of rice [54]. Likewise, the QNE 4 and cytochrome oxidase subunit 1 proteins of *P. cubensis* exhibited strong binding affinities with glucosyl flavones, terpenoids, and flavonoids from phytochemicals, antimicrobial compounds from botanicals (garlic and clove), and chemically synthesized compounds, suggesting the possibility of antifungal activity [55]. Moreover, four potential compounds (melianoninol, nimbinene, vilasinin, and fraxinellone) from *Melia azedarach* displayed considerable significant structural and pharmacological properties and could be probable antifungal drug candidates against *F. graminearum* [56].

Depending on the above circumstances, in silico work has a great impact on the world of plant science. So, computer-aided drug discovery has become a committed step of modern pathological advancement including plant disease management. *Nigrospora* spp. as a major phytopathological fungi has been targeted in the present study. Tef-1 has been selected as the target protein based on its structural and functional properties. Ten phytocompounds from two different sources were selected based on their antifungal activity. Seven out of ten showed higher binding affinity than the control in molecular docking (**Table 1**). These seven compounds did not violate any of the rules of Lipinski. Moreover, Andrograpanin from *Andrographis paniculata* and lawsaritol from *Lawsenia enermis* have the highest binding affinity than the other compounds of the same plant (−11.4 and −7.5 kcal mol^{-1}, respectively), forming hydrophobic interactions and hydrogen bonds with receptor protein amino acid residues and the RMSD values of both compounds were less than 3 which is considered a stable value. Furthermore, the RMSF value and the interactions of several bonds with the protein are comparatively close to the control fungicide carbendazim which indicates the ability of these compounds to be potential drug candidates against the protein [57].

Our recent studies on Nigrospora and plant-pathogen molecular modeling together provide a stronger framework for computational interpretation. Multi-locus phylogenies (ITS, TEF1-*α*, TUB2) have clarified that Nigrospora is a monophyletic Apiosporaceae genus with substantial hidden diversity and frequent roles as endophyte, saprobe, and plant pathogen, including newly described species from soil, cassava, Aquilaria and other hosts. Pathogenicity on economically important crops is now well documented, with leaf spot and blight caused by Nigrospora on olive, Camellia, bamboo and other plants verified through Koch's postulates and phylogeny-guided identification [58]. In parallel, best-practice workflows in plant-pathogen docking and MD emphasize careful target preparation, validation of homology models, benchmarking docking parameters, and routine use of MD (RMSD, RMSF, Rg, SASA, H-bond and free-energy analyses) to test complex stability and reduce false positives [59]. The outcomes of the present research suggest andrograpanin and lawsaritol as potential compounds to manage the Nigrospora leaf blight disease of guava. However, *in vitro* and field experiments are necessary to confirm these findings.

5. Conclusion

Nigrospora chinensis was found to be responsible for causing the leaf blight disease of guava. According to the evaluation of the effects of different physical parameters viz., culture media, temperature and pH, all have a regulatory effect on the fungal developments. Although we do not promote the use of synthetic fungicides for plant disease control, chemical fungicides and fungal antagonists can be potential candidates to reduce the disease loss. Furthermore, computer-aided virtual screening detected a number of phyto-compounds from selected plants having the potential to be biogenic fungicides against the disease in question. We

strongly believe that this study will serve as a valuable reference for the future investigations into the fungal diseases of guava.

Data Availability

All data supporting the results are included in the article.

Acknowledgements

This study was supported by a grant from Jahangirnagar University (JU), Dhaka, Bangladesh.

Conflicts of Interest

The authors of this research affirm that they have no competing interests concerning its publication.

References

[1] Hossain, A. and Badiuzzaman (2021) Hedonic Prices for the Fruit Market in Bangladesh: Lessons from Guava and Hog Plum Purchase Decisions. *Journal of Retailing and Consumer Services*, **62**, Article ID: 102636. https://doi.org/10.1016/j.jretconser.2021.102636

[2] Asim, M. and Alyas, T. (2025) Enhancing Guava Crop Health: A Computational Intelligence Approach to Disease Detection. *Journal of Innovative Computing and Emerging Technologies*, **5**, No. 1.

[3] Gayathri, S., Shanmugasundaram, K.A., Auxcilia, J., Shanthi, A., Karthikeyan, M. and Muthuvel, I. (2025) Exploring the Nutritional Value and Therapeutic Potential of Guava (*Psidium guajava* L.) Seeds and Leaves: Bioactive Compounds and Their Industrial Applications. *Annals of Phytomedicine*: *An International Journal*, **14**, 209-224. https://doi.org/10.54085/ap.2025.14.1.20

[4] Haque, M.N., Saha, B.K., Karim, M.R. and Bhuiyan, M.N.H. (1970) Evaluation of Nutritional and Physico-Chemical Properties of Several Selected Fruits in Bangladesh. *Bangladesh Journal of Scientific and Industrial Research*, **44**, 353-358. https://doi.org/10.3329/bjsir.v44i3.4410

[5] Alam, F., Islam, K.D. and Rahman, S.M. (2018) Variability among Selective Guava (*Psidium guajava* L.) Varieties Revealed by Morphology and RAPD Marker. *Jahangirnagar University Journal of Biological Sciences*, **7**, 89-98. https://doi.org/10.3329/jujbs.v7i2.40750

[6] Gupta, V.K. and Misra, A.K. (2012) *Fusarium chlamydosporum*, Causing wilt Disease of Guava (*Psidium guajava*L.) in India. *Archives of Phytopathology and Plant Protection*, **45**, 2425-2428. https://doi.org/10.1080/03235408.2012.728055

[7] Misra, A.K. (2017) Progressive Steps in Understanding and Solving Guava Wilt: A National Problem. *Indian Phytopathology*, **70**, 1-11. https://doi.org/10.24838/ip.2017.v70.i1.48983

[8] Honger, J.O., Amoatey, C.A., Bedu, I., Sackey, D.N., Agyekum, K.S., Coffie, S. and Otu, B. (2025) First Report of a Stylar End Rot Disease of Guava Fruits Caused by *Lasiodiplodia pseudotheobromae* in Ghana. *Physiological and Molecular Plant Pathology*, **142**, Article ID: 103051. https://doi.org/10.1016/j.pmpp.2025.103051

[9] Zakaria, L., Mazzura, W.C., Kong, W.H. and Baharuddin, S. (2012) Fusarium Species

Associated with Fruit Rot of Banana (Musa Spp.), Papaya (*Carica papaya*) and Guava (*Psidium guajava*). *Malaysian Journal of Microbiology*, **8**, 127-130. https://doi.org/10.21161/mjm.03812

[10] Pervez, Z., Alam, M.S., Islam, M.S., Ahmed, N.U. and Mahmud, M.R. (2018) First Report of Phytophthora Guava Fruit Rot in Bangladesh. *Journal of Plant Pathology & Microbiology*, **9**, 433. https://doi.org/10.4172/2157-7471.1000433

[11] Keith, L.M., Velasquez, M.E. and Zee, F.T. (2006) Identification and Characterization of Pestalotiopsis Spp. Causing Scab Disease of Guava, *Psidium guajava*, in Hawaii. *Plant Disease*, **90**, 16-23. https://doi.org/10.1094/pd-90-0016

[12] Mohamed, H. and Saad, A. (2009) The Biocontrol of Postharvest Disease (*Botryodiplodia theobromae*) of Guava (*Psidium guajava* L.) by the Application of Yeast Strains. *Postharvest Biology and Technology*, **53**, 123-130. https://doi.org/10.1016/j.postharvbio.2009.04.001

[13] Ji, C.Y., Ren, D.D., Liang, X.Y., Pan, F., Li, R.H., Lin, S., *et al.* (2023) First Report of *Nalanthamala psidii* Causing Wilt Disease of Guava in Guangdong, China. *Plant Disease*, **107**, Article No. 1943. https://doi.org/10.1094/pdis-05-22-1166-pdn

[14] Liao, Y.M., Wang, Z.X., Wei, M.C. and Wang, C. (2020) First Report of *Phyllosticta capitalensis* Causing Black Spot Disease on *Psidium guajava* in Mainland China. *Plant Disease*, **104**, Article No. 3252. https://doi.org/10.1094/pdis-02-20-0338-pdn

[15] Abdoula, R. and Ranghoo-Sanmukhiya, V.M. (2025) First Report of *Colletotrichum tropicale* Causing Anthracnose of *Psidium guajava* in Mauritius. *New Disease Reports*, **52**, e70072. https://doi.org/10.1002/ndr2.70072

[16] Zee, K.Y., Asib, N. and Ismail, S.I. (2021) First Report of *Lasiodiplodia theobromae* Causing Postharvest Fruit Rot on Guava (*Psidium guajava*) in Malaysia. *Plant Disease*, **105**, Article No. 2716. https://doi.org/10.1094/pdis-12-20-2732-pdn

[17] Ismail, S.I., Ahmad Dahlan, K., Abdullah, S. and Zulperi, D. (2021) First Report of *Neoscytalidium dimidiatum* Causing Fruit Rot on Guava (*Psidium guajava*) in Malaysia. *Plant Disease*, **105**, Article No. 220. https://doi.org/10.1094/pdis-06-20-1267-pdn

[18] Verweij, P.E., Snelders, E., Kema, G.H., Mellado, E. and Melchers, W.J. (2009) Azole Resistance in Aspergillus Fumigatus: A Side-Effect of Environmental Fungicide Use? *The Lancet Infectious Diseases*, **9**, 789-795. https://doi.org/10.1016/s1473-3099(09)70265-8

[19] Rahmani, A.H., Al Zohairy, M.A., Aly, S.M. and Khan, M.A. (2014) Curcumin: A Potential Candidate in Prevention of Cancer via Modulation of Molecular Pathways. *BioMed Research International*, **2014**, Article ID: 761608. https://doi.org/10.1155/2014/761608

[20] Nagoor Meeran, M.F., Javed, H., Al Taee, H., Azimullah, S. and Ojha, S.K. (2017) Pharmacological Properties and Molecular Mechanisms of Thymol: Prospects for Its Therapeutic Potential and Pharmaceutical Development. *Frontiers in Pharmacology*, **8**, Article No. 380. https://doi.org/10.3389/fphar.2017.00380

[21] Matasyoh, J.C., Kiplimo, J.J., Karubiu, N.M. and Hailstorks, T.P. (2007) Chemical Composition and Antimicrobial Activity of Essential Oil of *Tarchonanthus camphoratus*. *Food Chemistry*, **101**, 1183-1187. https://doi.org/10.1016/j.foodchem.2006.03.021

[22] Geiser, D.M., del Mar Jiménez-Gasco, M., Kang, S., Makalowska, I., Veeraraghavan, N., Ward, T.J., *et al.* (2004) FUSARIUM-ID V. 1.0: A DNA Sequence Database for Identifying Fusarium. *European Journal of Plant Pathology*, **110**, 473-479. https://doi.org/10.1023/b:ejpp.0000032386.75915.a0

[23] Ahmmed, M.S., Nisha, F.A. and Alam, N. (2022) First Report on Rhizome Rot Disease of *Curcuma longa* Caused by *Fusarium solani* in Bangladesh. *American Journal of Plant Sciences*, **13**, 506-516. https://doi.org/10.4236/ajps.2022.134033

[24] Kumar, S., Stecher, G., Li, M., Knyaz, C. and Tamura, K. (2018) MEGA X: Molecular Evolutionary Genetics Analysis across Computing Platforms. *Molecular Biology and Evolution*, **35**, 1547-1549. https://doi.org/10.1093/molbev/msy096

[25] Xue, Y., Shui, G. and Wenk, M.R. (2014) TPS1 Drug Design for Rice Blast Disease in Magnaporthe Oryzae. *SpringerPlus*, **3**, 1-9. https://doi.org/10.1186/2193-1801-3-18

[26] Nili, O., Azizi, A. and Abdollahzadeh, J. (2020) Development of an Efficient Tef-1α RNA Hairpin Structure to Efficient Management of *Lasiodiplodia theobromae* and *Neofusicoccum parvum*. Scientific Reports, **11**, Article No. 9612.

[27] UniProt Consortium (2018) UniProt: A Worldwide Hub of Protein Knowledge. *Nucleic Acids Research*, **47**, D506-D515. https://doi.org/10.1093/nar/gky1049

[28] Zhang, Y. (2008) Progress and Challenges in Protein Structure Prediction. *Current Opinion in Structural Biology*, **18**, 342-348. https://doi.org/10.1016/j.sbi.2008.02.004

[29] Shawan, M.M.A.K., Sharma, A.R., Halder, S.K., Arian, T.A., Shuvo, M.N., Sarker, S.R., *et al.* (2023) Advances in Computational and Bioinformatics Tools and Databases for Designing and Developing a Multi-Epitope-Based Peptide Vaccine. *International Journal of Peptide Research and Therapeutics*, **29**, Article No. 60. https://doi.org/10.1007/s10989-023-10535-0

[30] Mazumder, B., Ganguli, A., Akter, M.A., Al Arian, T., Shuvo, M.N., Mim, M.M., *et al.* (2026) *In Silico* Identification of Damaging CDK4 Variants Linked to Cancer Pathogenesis: Functional and Structural Insights. *Egyptian Journal of Medical Human Genetics*, **27**, Article No. 10. https://doi.org/10.1186/s43042-026-00843-7

[31] Cheng, T., Pan, Y., Hao, M., Wang, Y. and Bryant, S.H. (2014) Pubchem Applications in Drug Discovery: A Bibliometric Analysis. *Drug Discovery Today*, **19**, 1751-1756. https://doi.org/10.1016/j.drudis.2014.08.008

[32] O'Boyle, N.M., Banck, M., James, C.A., Morley, C., Vandermeersch, T. and Hutchison, G.R. (2011) Open Babel: An Open Chemical Toolbox. *Journal of Cheminformatics*, **3**, 1-14. https://doi.org/10.1186/1758-2946-3-33

[33] Morris, G.M., Huey, R., Lindstrom, W., Sanner, M.F., Belew, R.K., Goodsell, D.S., *et al.* (2009) Autodock4 and Autodocktools4: Automated Docking with Selective Receptor Flexibility. *Journal of Computational Chemistry*, **30**, 2785-2791. https://doi.org/10.1002/jcc.21256

[34] Goddard, T.D., Huang, C.C. and Ferrin, T.E. (2005) Software Extensions to UCSF Chimera for Interactive Visualization of Large Molecular Assemblies. *Structure*, **13**, 473-482. https://doi.org/10.1016/j.str.2005.01.006

[35] Khan, M.A., Al Mamun Khan, M.A., Mahfuz, A.M.U.B., Sanjana, J.M., Ahsan, A., Gupta, D.R., *et al.* (2022) Highly Potent Natural Fungicides Identified *in Silico* against the Cereal Killer Fungus Magnaporthe Oryzae. *Scientific Reports*, **12**, Article No. 20232. https://doi.org/10.1038/s41598-022-22217-w

[36] Tian, W., Chen, C., Lei, X., Zhao, J. and Liang, J. (2018) CASTp 3.0: Computed Atlas of Surface Topography of Proteins. *Nucleic Acids Research*, **46**, W363-W367. https://doi.org/10.1093/nar/gky473

[37] Ferreira, L., Dos Santos, R., Oliva, G. and Andricopulo, A. (2015) Molecular Docking and Structure-Based Drug Design Strategies. *Molecules*, **20**, 13384-13421. https://doi.org/10.3390/molecules200713384

[38] Sharma, S., Sharma, A. and Gupta, U. (2021) Molecular Docking Studies on the Anti-

fungal Activity of *Allium sativum* (Garlic) against Mucormycosis (Black Fungus) by BIOVIA Discovery Studio Visualizer 21.1. 0.0. *Annals of Antivirals and Antiretrovirals*, **5**, 28-32.

[39] Trott, O. and Olson, A.J. (2009) AutoDock Vina: Improving the Speed and Accuracy of Docking with a New Scoring Function, Efficient Optimization, and Multithreading. *Journal of Computational Chemistry*, **31**, 455-461. https://doi.org/10.1002/jcc.21334

[40] Daina, A., Michielin, O. and Zoete, V. (2017) SwissADME: A Free Web Tool to Evaluate Pharmacokinetics, Drug-Likeness and Medicinal Chemistry Friendliness of Small Molecules. *Scientific Reports*, **7**, Article No. 42717. https://doi.org/10.1038/srep42717

[41] Lipinski, C.A. (2004) Lead- and Drug-Like Compounds: The Rule-of-Five Revolution. *Drug Discovery Today*: *Technologies*, **1**, 337-341. https://doi.org/10.1016/j.ddtec.2004.11.007

[42] Wang, M., Liu, F., Crous, P.W. and Cai, L. (2017) Phylogenetic Reassessment of Nigrospora: Ubiquitous Endophytes, Plant and Human Pathogens. *Persoonia-Molecular Phylogeny and Evolution of Fungi*, **39**, 118-142. https://doi.org/10.3767/persoonia.2017.39.06

[43] Shuvo, M.N., Halder, S.K., Alam, N., Himel, M.K. and Shil, A. (2024) Developing Phytocompound-Based New Drugs against Multi-Drug-Resistant *Staphylococcus aureus*. *Royal Society Open Science*, **11**, Article ID: 231475. https://doi.org/10.1098/rsos.231475

[44] Qin, S., Chen, X., Zhou, X., Zhao, J., Baccelli, I. and Cernava, T. (2021) First Report of Camellia Oleifera Leaf Blight Caused by *Nigrospora chinensis*. *Journal of Plant Pathology*, **103**, 711-712. https://doi.org/10.1007/s42161-021-00793-6

[45] Ahmmed, M.S., Sikder, M.M., Sultana, A. and Alam, N. (2022) First Report of Leaf Spot Disease of Aloe Vera Caused by *Nigrospora sphaerica* in Bangladesh. *Journal of Plant Sciences*, **17**, 95-101. https://doi.org/10.3923/jps.2022.95.101

[46] Sempere, F. and Santamarina, M.P. (2006) Microscopic and Macroscopic Study of the Interaction *Betweenalternaria alternata* (fr.) Keissler and *Nigrospora oryzae* (Berk. & Broome) Petch. *Annals of Microbiology*, **56**, 101-107. https://doi.org/10.1007/bf03174989

[47] Zheng, X.R., Liu, C.L., Zhang, M.J., Shang, X.L., Fang, S.Z. and Chen, F.M. (2021) First Report of Leaf Blight of *Cyclocarya paliurus* Caused by *Nigrospora sphaerica* in China. *Crop Protection*, **140**, Article ID: 105453. https://doi.org/10.1016/j.cropro.2020.105453

[48] Yadav, M., Sharma, S., Singh, S.P., Tiwari, N.N., Kumar, A. and Yadav, S. (2025) *In Vitro* Efficacy of Different Pesticides against *C. falcatum* Causing Red Rot in Sugarcane. *Agrica*, **14**, 55-58. https://doi.org/10.5958/2394-448x.2025.00005.3

[49] Mahmoud, E.E., Hussien, Z., Ibrahim, M. and Abdel-Gayed, M. (2016) Compatibility between Chemical Inducers and Amistar Top Fungicide for Controlling Onion Downy Mildew and Purple Blotch Diseases. *Egyptian Journal of Phytopathology*, **44**, 67-84. https://doi.org/10.21608/ejp.2016.91536

[50] Baria, T.T. and Rakholiya, K.B. (2020) Evaluation of the Efficacy of Different Fungicides against *Fusarium musae*, a Fruit Rot Disease of Banana. *Annual Research & Review in Biology*, **35**, 212-219. https://doi.org/10.9734/arrb/2020/v35i1230326

[51] Liu, Y., An, J., Safdar, A., Shen, Y., Sun, Y., Shu, W., *et al.* (2024) Identification and Characterization of Nigrospora Species and a Novel Species, *Nigrospora anhuiensis*, Causing Black Leaf Spot on Rice and Wild Rice in the Anhui Province of China. *Jour-*

nal of Fungi, **10**, Article No. 156. https://doi.org/10.3390/jof10020156

[52] Walke, S.J., Jagtap, G.P., Lohakare, A.S., Ramteke, R.A. and Dhore, Y.P. (2024) To Evaluate *in Vitro* Efficacy of Different Fungicides against *Pyricularia grisea* (Cooke) Sacc. Causing Blast of Pearl Millet [*Pennisetum glaucum* (L.) R. Br]. *International Journal of Advanced Biochemistry Research*, **8**, 240-243. https://doi.org/10.33545/26174693.2024.v8.i2sd.542

[53] Swathy, K., Nisha, V. and Vivekanandhan, P. (2024) Biological Control Effect of *Trichoderma harzianum* (Hypocreales: Hypocreaceae) against Phytopathogens. *Environmental Quality Management*, **34**, Article No. 22227. https://doi.org/10.1002/tqem.22227

[54] Joshi, T., Pandey, S.C., Maiti, P., Tripathi, M., Paliwal, A., Nand, M., *et al.* (2021) Antimicrobial Activity of Methanolic Extracts of *Vernonia cinerea* against *Xanthomonas oryzae* and Identification of Their Compounds Using *in Silico* Techniques. *PLOS ONE*, **16**, e0252759. https://doi.org/10.1371/journal.pone.0252759

[55] Jhansirani, N., Devappa, V., Sangeetha, C.G., Sridhara, S., Shankarappa, K.S. and Mohanraj, M. (2023) Identification of Potential Phytochemical/Antimicrobial Agents against *Pseudoperonospora cubensis* Causing Downy Mildew in Cucumber through *In-Silico* Docking. *Plants*, **12**, Article No. 2202. https://doi.org/10.3390/plants12112202

[56] Joshi, T., Joshi, T., Sharma, P., Pundir, H. and Chandra, S. (2020) *In Silico* Identification of Natural Fungicide from *Melia azedarach* against Isocitrate Lyase of *Fusarium graminearum*. *Journal of Biomolecular Structure and Dynamics*, **39**, 4816-4834. https://doi.org/10.1080/07391102.2020.1780941

[57] Halder, S.K., Sultana, I., Shuvo, M.N., Shil, A., Himel, M.K., Hasan, M.A., *et al.* (2023) *In Silico* Identification and Analysis of Potentially Bioactive Antiviral Phytochemicals against SARS-CoV-2: A Molecular Docking and Dynamics Simulation Approach. *BioMed Research International*, **2023**, Article ID: 5469258. https://doi.org/10.1155/2023/5469258

[58] Hao, Y., Aluthmuhandiram, J.V.S., Chethana, K.W.T., Manawasinghe, I.S., Li, X., Liu, M., *et al.* (2020) Nigrospora Species Associated with Various Hosts from Shandong Peninsula, China. *Mycobiology*, **48**, 169-183. https://doi.org/10.1080/12298093.2020.1761747

[59] Naimuzzaman, M., Hasan, M.M., Kumer, A., Hossin, A.Y., Harun-Ur-Rashid, M., Roy, S.K., *et al.* (2025) Computational and *in Silico* Study of Novel Fungicides against Combating Root Rot, Gray Mold, Fusarium Wilt, and Cereal Rust. *PLOS ONE*, **20**, e0316606. https://doi.org/10.1371/journal.pone.0316606